JOURNAL OF COMPUTATIONAL PHYSICS **142,** 506–520 (1998)
ARTICLE NO. CP985951

A Hybrid Numerical Method for Loaded Highly Resonant Single Mode Cavities

Cheryl V. Hile and Gregory A. Kriegsmann

Department of Mathematics, Center for Applied Mathematics and Statistics, New Jersey Institute of Technology, University Heights, Newark, New Jersey 07102

Received April 21, 1997; revised December 10, 1997

We describe a hybrid numerical method for modeling the electromagnetic interaction of a low-loss ceramic material in a single-mode waveguide applicator. The method we propose utilizes a combination of asymptotic and numerical techniques. The interaction between the applicator and the electromagnetic fields is described using scattering matrix theory and the interaction between the electromagnetic fields and the ceramic is determined numerically. Several simulations, including a low-loss slab and low-loss post, are presented to show the accuracy and simplicity of this method along with the relatively small amount of computer resources it requires.

1. INTRODUCTION

Over the last several the years, the use of microwave energy to sinter or join a wide variety of ceramic materials has become an important technology. This technology has the capability of producing high quality materials efficiently because heat is generated rapidly within the material instead of diffusing slowly into its surface. However, this technology cannot be utilized to its full potential without a more fundamental understanding of the complicated interaction between the waveguide applicator, the electromagnetic fields, and the ceramic. Detailed knowledge of this interaction will lead to a more complete characterization of the heating process and thereby help to prevent nonuniform heating and lead to future optimizations of the heating process.

The challenge of obtaining this detailed knowledge is computationally daunting; the time harmonic Maxwell's equations are coupled in a highly nonlinear manner to the heat equation. The nonlinearities are threefold. The first is the dependence of the effective conductivity σ on the temperature. The second is the source term $\sigma|\mathbf{E}|^2$ in the heat equation, where $\mathbf{E}$ is the electric field in the material. The third is the thermal boundary condition on the surface of the material; it is proportional to the fourth power of the temperature. In

0021-9991/98 $25.00

the absence of any simplifications (e.g., small sample, small Biot number, etc.) the only recourse is to numerically solve these equations in a marching manner: First, the effective conductivity is computed from the initial temperature distribution. Second, Maxwell's equations are solved numerically. Third, the heat equation is marched forward one time step using another numerical method. The effective conductivity is computed at the new temperature distribution and the process is continued. This iteration procedure continues until a steady temperature is obtained or until thermal runway occurs and the sample is damaged.

A numerical technique frequently used to solve the electromagnetic portion of the marching scheme is the finite difference time domain (FDTD) method [1–3, 17, 18]. This method is used extensively in computational electromagnetics because it is relatively easy to implement and requires no matrix storage or inversions. The technique is based upon the limiting amplitude principal [4] which states that an incident time harmonic wave ultimately produces a time harmonic response. The FDTD method exploits this principal in an explicit fashion: the numerical solution starts with an arbitrary initial condition and is stepped forward in time until a time harmonic response is obtained. In the context of microwave heating of ceramic materials, the convergence rate of this technique depends upon the amount of electromagnetic energy absorbed by the ceramic target and upon the time required for the transient electromagnetic fields to radiate out of the waveguide applicator. Consequently, this technique works effectively for lossy ceramics, which readily absorb electromagnetic energy, and for low Q cavities, where the transient electromagnetic fields radiate out of the cavity rather quickly.

Other numerical methods, such as finite element (FE) algorithms [5, 6], are also used to solve the time harmonic Maxwell's equations. These elliptic solvers require the construction and numerical inversion of large matrices. For low Q cavities and lossy ceramics the resulting matrices are well conditioned.

In many important applications, the ceramic is a low loss material which absorbs only a small amount of electromagnetic energy. Consequently, the cavity must have a high Q to allow the electromagnetic fields to build up sufficient strength to heat the ceramic. This scenario makes both the FDTD and FE methods inefficient. For the FDTD method, the electromagnetic fields become trapped within the cavity and the transients are forced to linger for many periods before radiating out of the structure. This dramatically increases the time needed for the fields to converge to a time harmonic steady state. For the FE method, the resulting matrices become highly ill-conditioned because of a near resonant state. Either technique can still provide a detailed description of the electromagnetic-material interaction, but both will require more extensive computer resources. This is especially true when parameter studies are needed to deduce trends and functional relationships.

In this paper we focus on the electromagnetic aspects of the heating problem. Specifically, we develop a hybrid numerical method for describing the interaction of an electromagnetic wave with a low loss ceramic material in a high Q cavity. The method we propose utilizes a combination of asymptotic and numerical techniques. The asymptotic aspects are based upon scattering matrix theory, which assumes that the evanescent modes excited by the iris have a negligible effect on the ceramic, and the evanescent modes generated by the ceramic have a negligible effect on the iris. These assumptions are guaranteed in microwave applicators by carefully choosing the location of the ceramic and the size of the cavity. However, in other applications, such as optical resonators and couplers, these evanescent waves play a crucial role [7].

The use of scattering matrix theory allows us to decompose the electromagnetic problem into two independent pieces. The first requires the computation of the reflection coefficient for an iris in an infinite homogeneous waveguide. This problem is classical and there are many excellent approximations to its solution [8]. The second requires the computation of the electromagnetic fields for a ceramic target in an infinite homogenous waveguide with a short located at $Z = L$. Because there is little resonant character to this problem, it is not ill-conditioned and any accurate numerical method can be used to approximate its solutions. Both the FDTD and FE methods are excellent candidates. The solutions of these two pieces are then analytically combined using a simple formula to produce an accurate approximation to the original problem. The result is an efficient and accurate hybrid method.

We note that for a given aperture opening and frequency, our hybrid method requires an extremely accurate approximation of the resonant length L of the cavity. The determination of this critical length is a difficult problem in itself and has been addressed by other authors [9, 10]. The technique we develop is along similar lines and requires a single numerical (e.g., FDTD) calculation for a sample in an infinite and homogeneous waveguide, and an approximation to the reflection coefficient for an iris. We also note that a straightforward application of the FDTD method to the loaded cavity problem possesses a similar problem. For this case, the length of the cavity and the aperture are fixed and the resonant frequency must be determined. This can be done effectively by obtaining the distorted wavelength of the field in the loaded cavity and backing out the perturbed eigenfrequency [11].

We observe here that our splitting of the elliptic scattering problem into two pieces is similar in spirit to domain decomposition techniques [12]. However, these techniques require an iteration procedure that connects all the sub-domains; our connection is done analytically. If the FDTD method is used to numerically obtain time harmonic solutions to our two independent problems, then our technique bears some resemblance to the FDTD diakoptic method [13, 14]. However, this technique requires time domain convolutions for connecting the sub-regions of the structure. This is not required for our hybrid method as we analytically combine the two time harmonic solutions.

The outline of this paper is as follows. In Section 2, the problem of the interaction of an incident microwave mode with an arbitrary cylindrical, low-loss ceramic in a TE_{103} waveguide applicator is presented. In Section 3, scattering matrix theory is used to describe the interaction between the applicator, the incident electromagnetic field, and the electromagnetic field reflected by the ceramic. In Section 4, the FDTD method is used to determine the interaction between the electromagnetic fields, the ceramic, and the short in the absence of the iris. In Section 5, two example problems are presented to demonstrate the accuracy and computational efficiency of this hybrid method. Finally, in Section 6, a method for computing resonant lengths is described.

2. FORMULATION

A ceramic sample of arbitrary cylindrical shape occupies a portion of a TE_{103} waveguide, shown in Fig. 1. The applicator is comprised of a waveguide, a symmetric iris, and a movable back wall, called a short. The cavity and its load are excited by the incident TE_{10} mode

$$\mathbf{E}_{inc} = E_0 e^{iK_1 Z} \sin(\pi X/W)\hat{\mathbf{Y}} \tag{1a}$$

$$\mathbf{H}_{inc} = E_0 e^{iK_1 Z}\left[\frac{K_1}{\mu_0\omega}\sin(\pi X/W)\hat{\mathbf{X}} - \frac{i\pi}{W\mu_0\omega}\cos(\pi X/W)\hat{\mathbf{Z}}\right], \tag{1b}$$

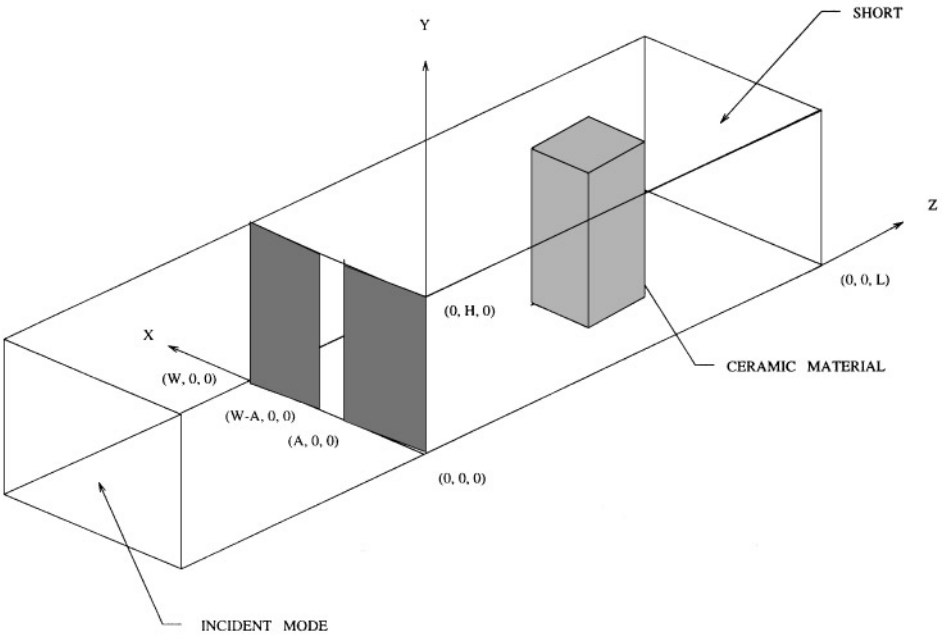

FIG. 1. TE_{103} waveguide applicator with an arbitrary cylindrical ceramic material.

where E_0 is the strength of the incident mode, $K_1 = \sqrt{\omega^2/c^2 - \pi^2/W^2}$ is the wave number of the propagating mode, ω is the source frequency, c is the speed of light in a vacuum, μ_0 is the magnetic permeability of free space, and W is the width of the guide. The time harmonic electromagnetic fields in the applicator are described by Maxwell's equations,

$$\nabla \times \mathbf{E} = i\omega\mu_0\mathbf{H}, \tag{2a}$$

$$\nabla \times \mathbf{H} = -i\omega\epsilon\mathbf{E} + \sigma\mathbf{E}, \tag{2b}$$

where ϵ, the effective permittivity, is a function of position. Outside the sample $\epsilon = \epsilon_0$, the permittivity of free-space. Inside the sample $\epsilon = \epsilon_R$, the real effective electrical permittivity. The effective electrical conductivity, σ, takes the electrical losses of the material into account.

The electromagnetic fields satisfy boundary conditions which follow from Maxwell's equations and from the assumption that the waveguide walls and iris are perfectly conducting. These conditions are written as

$$\mathbf{E} \times \mathbf{n} = 0, \tag{3}$$

and correspond to the tangential components of the electric field vanishing on the waveguide walls and iris. In addition, the tangential components of the electric and magnetic fields must be continuous across the surface of the sample. Specifically, we have

$$[\mathbf{H} \times \mathbf{n}]_S = 0, \tag{4a}$$

$$[\mathbf{E} \times \mathbf{n}]_S = 0, \tag{4b}$$

where $[\ ]_S$ denotes the jump across the sample surface S.

Finally, the waveguide feeding the cavity is assumed to support only a TE_{10} mode. Thus, for $Z \ll 0$ the electric field takes the form

$$\mathbf{E} = E_0[e^{iK_1Z} + R_0 e^{-iK_1Z}]\sin(\pi X/W)\hat{\mathbf{Y}}, \tag{5}$$

where R_0 is the amplitude of the reflected mode. The magnetic field is given by a similar expression.

For convenience in the analysis which follows, we introduce the dimensionless variables and parameters,

$$\tilde{\mathbf{E}} = \mathbf{E}/E_0, \qquad \tilde{\mathbf{H}} = \mathbf{H}/(\sqrt{\epsilon_0/\mu_0}E_0), \qquad (x, y, z) = (X, Y, Z)/W, \tag{6a}$$

$$(l, h, a) = (L, H, A)/W, \qquad t = \omega T, \qquad k_1 = K_1 W. \tag{6b}$$

The problem now at hand is to find $\tilde{\mathbf{E}}$ and $\tilde{\mathbf{H}}$ that satisfy the equations

$$\nabla \times \tilde{\mathbf{E}} = ik\tilde{\mathbf{H}}, \tag{7a}$$

$$\nabla \times \tilde{\mathbf{H}} = -ik\tilde{\mathbf{E}} + \frac{\sigma k}{\omega\epsilon}\tilde{\mathbf{E}}, \tag{7b}$$

in the region $(-\infty < z < l)$ and take the asymptotic form

$$\tilde{\mathbf{E}} = [e^{ik_1 z} + R_0 e^{-ik_1 z}]\sin(\pi x)\hat{\mathbf{y}}, \tag{8a}$$

$$\tilde{\mathbf{H}} = \frac{k_1}{k}[e^{ik_1 z} - R_0 e^{-ik_1 z}]\sin(\pi x)\hat{\mathbf{x}} + -i\frac{\pi}{k}[e^{ik_1 z} + R_0 e^{-ik_1 z}]\cos(\pi x)\hat{\mathbf{z}}, \tag{8b}$$

far away from the iris ($z \ll 0$). The index of refraction is defined as $n^2 = \epsilon/\epsilon_0$, the dimensionless wave number by $k = \omega W/c$, and the dimensionless propagation constant by $k_1 = K_1 W$. These equations are subject to the boundary conditions described above. Together they form an elliptic boundary value problem on an infinite domain which cannot be solved analytically, even for simply shaped targets.

We observe here that for a given aperture and frequency, the cavity will be highly resonant, for discrete values of l. These values are difficult to obtain for an arbitrary target. In Section 6 we describe a method which accurately and explicitly estimates these critical lengths.

3. THE ASYMPTOTIC METHOD

The basic idea behind the analysis that follows is to mathematically remove the iris from the problem. We do this by applying scattering matrix theory to describe the interactions of the iris with the incident electromagnetic field and with the electromagnetic field reflected by the ceramic sample and the short. This theory is asymptotic in character, as it neglects the evanescent modes excited by the iris and ceramic sample.

We begin by placing an imaginary plane, labeled z_I in Fig. 2, between the iris and the cylindrical target. The position z_I is chosen so that the evanescent modes generated by the iris and the cylinder are negligible. The field at this plane is given by

$$\tilde{\mathbf{E}}_I = [T_1 e^{ik_1 z} + E_1 e^{-ik_1 z}]\sin(\pi x)\hat{\mathbf{y}}, \tag{9}$$

where T_1 and E_1 are unknown at this point in time.

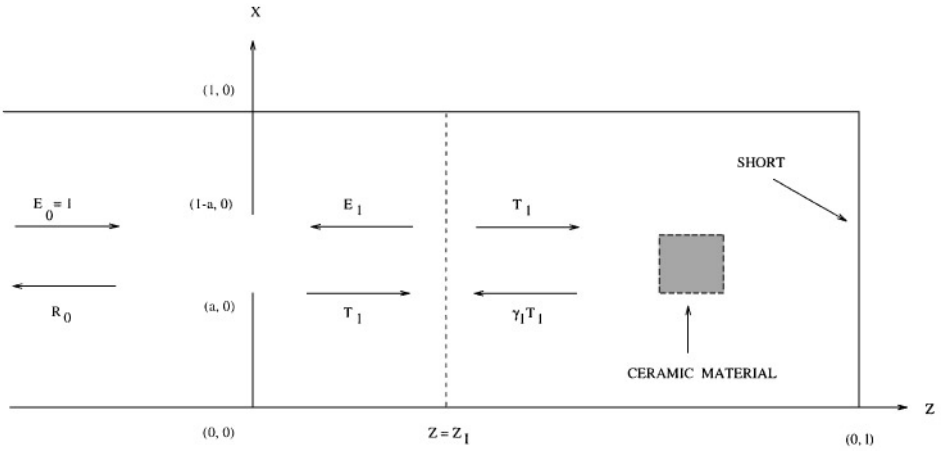

FIG. 2. Scattering matrix schematic for a TE_{103} waveguide applicator.

We next focus our attention on the region $z < z_I$, which contains only the iris. The iris is irradiated by two propagating modes. The first comes from the source, i.e., the first term in (8a). The second mode is produced by the scattering from the cylinder and short, i.e., the second term in (9). The iris appears to reflect a mode to the left, i.e., the second term in (8a), and a mode to the right, i.e., the first term in (9). These coefficients are related by the linear equations

$$R_0 = r_1(a) + (1 + r_1(a))E_1, \tag{10a}$$

$$T_1 = (1 + r_1(a)) + r_1(a)E_1, \tag{10b}$$

where the matrix is called the scattering matrix for the iris. The matrix element $r_1(a)$ is the reflection coefficient for an iris in an infinite and homogeneous waveguide and $1 + r_1(a)$ is the corresponding transmission coefficient. These coefficients depend upon the iris height, a, and the dimensionless wave number k. Approximations for r_1 are given in many standard texts, one of which is [8]

$$r_1(a, k) = \frac{-iS}{1 + iS}, \tag{11a}$$

$$S = S(a, k) = \frac{\pi}{k_1}\left[\tan^2(\pi a) - \frac{3\delta_3 \sin^4(\pi a)}{1 - \delta_3 \cos^2(\pi a)}\right], \tag{11b}$$

$$\delta_3 = \sqrt{1 - \frac{k^2}{9\pi^2}}. \tag{11c}$$

We next focus our attention on the region to the right of the plane, $z > z_I$. The first term in Eq. (9) can be interpreted as an incident mode of strength T_1 which impinges upon the cylindrical target and the short. The second term in Eq. (9) is the wave reflected by this structure. The amplitude of this wave is related to T_1 by $E_1 = \gamma_1 T_1$. The reflection coefficient γ_1 is the amplitude of the reflected mode caused by a unit incident field upon the ceramic sample and the short *without the iris*. Inserting this relationship into Eq. (10b) we obtain

$$T_1 = \frac{1 + r_1(a)}{1 - r_1(a)\gamma_1}. \tag{12}$$

Inserting these results into (10a) we find the amplitude of the reflected mode

$$R_0 = r_1(a) + (1 + r_1(a))\gamma_1 \left[\frac{1 + r_1(a)}{1 - r_1(a)\gamma_1} \right]. \tag{13}$$

These equations show the explicit dependence of T_1 and R_0 upon the iris height a and reflection coefficient γ_1.

Finally, we summarize the above results. According to our approximation, the ceramic sample is essentially irradiated by a TE_{10} mode of strength T_1. This mode can be thought of as propagating in an infinite and homogeneous guide until it interacts with the cylinder and short to produce a reflected wave. This reflected mode is of strength $\gamma_1 T_1$. The effects of the iris are contained in T_1 and R_0.

To complete the description of our method we define

$$\mathbf{e} = \tilde{\mathbf{E}}/T_1, \qquad \text{and} \qquad \mathbf{h} = \tilde{\mathbf{H}}/T_1, \tag{14}$$

which satisfy Maxwell's equations. The boundary conditions on the lateral walls of the waveguide, on the short, and across the sample are the same as before. However, we now have for $z \ll 0$

$$\mathbf{e} = [e^{ik_1 z} + \gamma_1 e^{-ik_1 z}] \sin(\pi x)\hat{\mathbf{y}}, \tag{15a}$$

$$\mathbf{h} = \frac{k_1}{k}[e^{ik_1 z} - \gamma_1 e^{-ik_1 z}] \sin(\pi x)\hat{\mathbf{x}} + -i\frac{\pi}{k}[e^{ik_1 z} + \gamma_1 e^{-ik_1 z}] \cos(\pi x)\hat{\mathbf{z}}. \tag{15b}$$

The electromagnetic boundary value problem we must solve is Eq. (7) for $\mathbf{e}$ and $\mathbf{h}$ throughout the entire waveguide *without the iris*. Once this is done, γ_1 is deduced from Eq. (15), which allows T_1 to be obtained from Eq. (12) and R_0 to be obtained from Eq. (13). The electric field $\tilde{\mathbf{E}}$ is then obtained from Eq. (14).

4. NUMERICAL METHOD

We use the finite difference time domain (FDTD) method to solve Eq. (7) throughout the entire waveguide without the iris, shown in Fig. 3. The electromagnetic fields are written

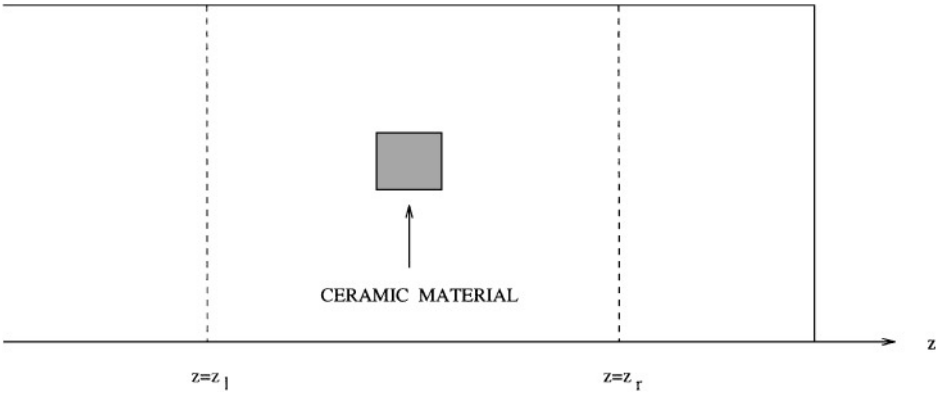

FIG. 3. FDTD computational domain for hybrid method.

there as

$$\mathbf{e} = E_y(x, z, t)\mathbf{y},$$
$$\mathbf{h} = H_x(x, z, t)\mathbf{x} + H_z(x, z, t)\mathbf{z}.$$

Accordingly, Eqs. (7) are replaced by the time dependent equations

$$\frac{\partial H_x}{\partial t} = \frac{1}{k}\frac{\partial E_y}{\partial z}, \tag{16a}$$
$$\frac{\partial H_z}{\partial t} = -\frac{1}{k}\frac{\partial E_y}{\partial x}, \tag{16b}$$
$$\frac{\partial E_y}{\partial t} = \frac{1}{k\epsilon}\left(\frac{\partial H_x}{\partial z} - \frac{\partial H_z}{\partial x}\right) - \sigma E_y. \tag{16c}$$

The electric and magnetic fields are evaluated alternatively at half time steps ($n\Delta t$ and $(n + 1/2)\Delta t$) and the spatial coordinates (x, z) are positioned at $(i\Delta, j\Delta)$:

$$H_x^{n+1/2}(i, j) = H_x^{n-1/2}(i, j) + \frac{\Delta t}{k\Delta}\left(E_y^n(i, j+1) - E_y^n(i, j)\right) \tag{17a}$$
$$H_z^{n+1/2}(i, j) = H_z^{n-1/2}(i, j) - \frac{\Delta t}{k\Delta}\left(E_y^n(i+1, j) - E_y^n(i, j)\right) \tag{17b}$$
$$E_y^{n+1}(i, j) = \left[\left(1 - \frac{\sigma\Delta t}{2}\right)E_y^n(i, j) + \frac{\Delta t}{k\epsilon\Delta}\left(H_x^{n+1/2}(i, j) - H_x^{n+1/2}(i, j-1)\right.\right.$$
$$\left.\left. - H_z^{n+1/2}(i, j) + H_z^{n+1/2}(i-1, j)\right)\right] \Big/ \left(1 + \frac{\sigma\Delta t}{2}\right). \tag{17c}$$

To truncate our computational domain we apply a mode killing, non-reflecting boundary operator to the total electric field on the plane $z_l = -l$. Choosing l large enough assures us that the evanescent waves are negligible. It follows from the operators presented in Ref. [15] that

$$\frac{\partial E_y}{\partial z} - k_1\frac{\partial E_y}{\partial t} = 2ik_1 e^{i(k_1 z_l - t)}\sin(\pi x). \tag{18}$$

This operator allows incident waves to propagate to the right (into the computational domain) and annihilates the reflected mode which propagates to the left (out of the computational domain). Higher order boundary operators are derived in [15], but we shall not pursue them here.

In discretized form Eq. (18) is written as

$$E_y^{n+1}(1, j) = E_y^{n-1}(1, j) - \frac{\Delta t}{k_1\Delta}\left(E_y^n(0, j) - E_y^n(2, j)\right) - 4i\Delta t e^{i(k_1\Delta - n\Delta t)}\sin(\pi j\Delta). \tag{19}$$

To obtain an expression for $E_y^n(0, j)$, a point outside the computational domain, we discretize the following nondimensional wave equation, centered at $(1, j)$,

$$\frac{\partial^2 E_y}{\partial t^2} = \frac{1}{k^2}\left(\frac{\partial^2 E_y}{\partial x^2} + \frac{\partial^2 E_y}{\partial x^2}\right). \tag{20}$$

This provides the following expression for the left boundary condition:

$$E_y^{n+1}(1,j) = \Bigg[-E_y^{n-1}(1,j) + 2E_y^n(1,j) + \left(\frac{\Delta t}{k\Delta}\right)^2 \big(2E_y^n(2,j) - 4E_y^n(1,j) \tag{21}$$

$$+ E_y^n(1,j+1) + E_y^n(1,j-1) + \frac{k_1\Delta}{\Delta t} E_y^{n-1}(1,j) - 4ik_1\Delta e^{i(k_1\Delta - n\Delta t)}$$

$$\times \sin(\pi j\Delta)\big)\Bigg] \Bigg/ \left(1 + \frac{k_1\Delta t}{k^2\Delta}\right). \tag{22}$$

On the surface of the ceramic, the boundary conditions from Eq. (4) require that the tangential components of the electric and magnetic fields be continuous. We satisfy these conditions by using average values for the permittivity on the boundary points of the ceramic. Finally, we prescribe $E_y = 0$ on the short $z = z_r$.

5. SIMULATIONS

To demonstrate the accuracy and computational efficiency of this hybrid numerical method, we present two example problems. The first is concerned with the microwave interaction with a slab which completely fills the cross-section of the waveguide. In the second, a cylinder is placed in the guide as shown in Fig. 1. For each case we have fixed the microwave frequency at $f = 2.45 \times 10^9$ Hz, the width of the waveguide at $W = 109.22$ mm, and the iris height at $A = 17.5$ mm. This gives us $k = 5.6$ and $a = 0.42$. In each example we must specify a resonant length l. When the sample is a slab, an approximate formula has been presented in Ref. [16]. When the sample is a post, the method presented in the following section is used. For both cases we use the FDTD scheme to numerically solve Eqs. (16) for the scaled fields **e** and **h**. The iris is not present in these calculations. Once the reflection coefficient γ_1 and **e** are determined numerically, the electric field is obtained from $\tilde{\mathbf{E}} = T_1\mathbf{e}$, where T_1 is given by Eq. (12). Finally, we took $\Delta = l/800$, $\Delta t = k\Delta/\sqrt{2}$, and $z_l = 0$.

We consider in our first example a slab of width 20.8 mm whose center is placed at $Z = 110$ mm. The resonant length for this case is $L = 241.5$ mm ($l = 2.21$) which-corresponds to the TE_{103} mode for the closed cavity. The length, l, of the cavity is chosen to maximize the electric field of the cavity if the sample is loss-less.

Figure 4 shows the amplitude of the electric field, E_y, throughout the waveguide applicator when the effective electrical conductivity, σ, equals 0. The dimensionless incident electric field has a strength of one and the maximum of the electric field in the cavity is 36. This shows the resonant character of the applicator. Figure 5 shows the maximum of the electric field for three different values of electrical conductivity ($\sigma = 0.0$, $\sigma = 0.001$, and $\sigma = 0.01$). It is readily apparent from these simulations that increasing the conductivity, while keeping the length l fixed, produces smaller fields. This is a detuning effect which is characteristic of high Q cavities.

The convergence times (in CPU minutes on a SGI Indigo2 Impact R10000 workstation) for these three cases were 70, 40, and 15 min, respectively. We realize that these convergence times are large for the simple geometry we are considering. This is because a fine mesh (i.e., small Δ) is needed for the stringent converge of the electromagnetics fields to ensure that the cavity is resonant. To check these results and compare convergence times, we applied the FDTD to the same scattering problem with the iris present. The results were identical to

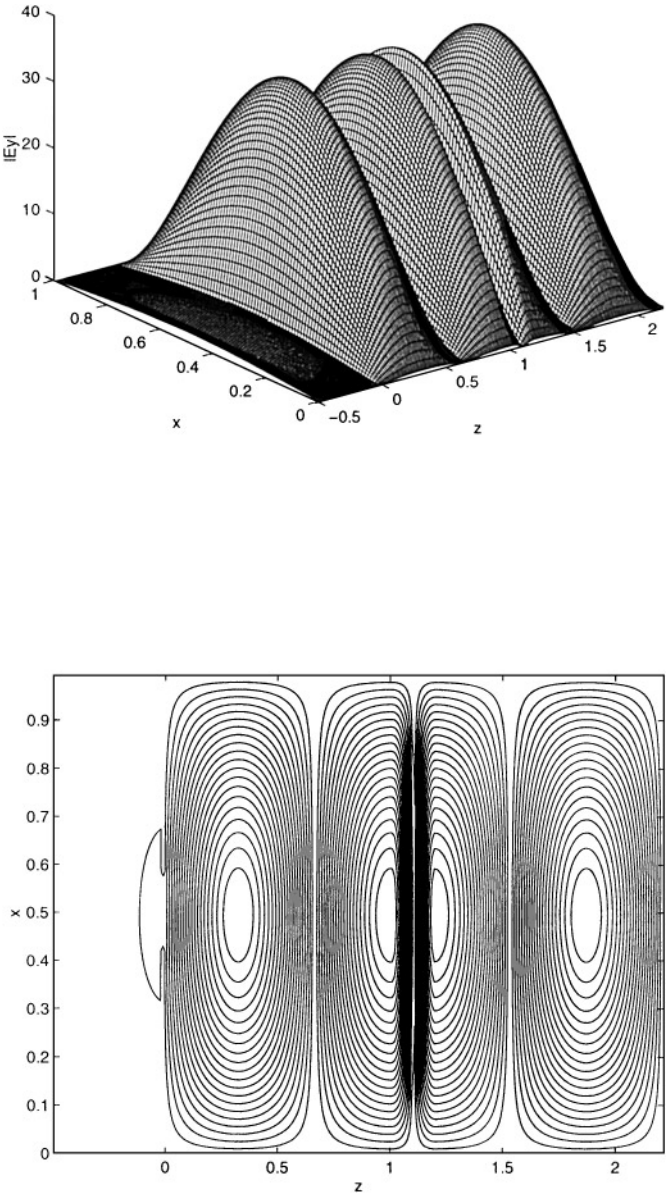

FIG. 4. Amplitude of E_y throughout the TE_{103} waveguide applicator containing a slab with $\sigma = 0$.

the hybrid method. However, the convergence times for these simulations were 405, 210, and 80 min, respectively, a factor of roughly six times slower.

We consider in our second example a square post of width 41.5 mm whose center is placed at $X = 54.6$ mm and $Z = L/2$, as shown in Fig. 1. The resonant length is determined using the method presented in the following section. It required one numerical simulation using the FDTD scheme to determine the required scattering matrix (i.e., to compute r_c and t_c). This preliminary calculation took 55 CPU min (approximately one tenth the time of the hybrid calculation). The resonant length for this case is $L = 279.7$ mm ($l = 2.56$) which corresponds to the TE_{103} mode for the closed cavity. The length, l, of the cavity is chosen to maximize the electric field of the cavity if the sample is loss-less.

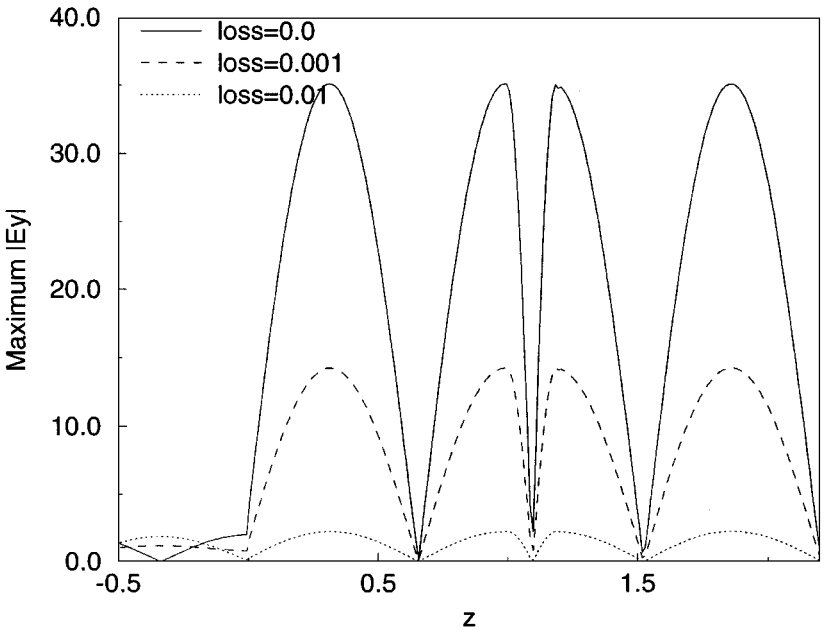

FIG. 5. Maximum amplitude of E_y throughout the TE_{103} waveguide applicator with containing a slab with $\sigma = 0.0$, $\sigma = 0.001$, and $\sigma = 0.01$.

Figure 6 shows the amplitude of the electric field, E_y, throughout the waveguide applicator when the effective electrical conductivity $\sigma = 0$. The dimensionless incident electric field has a strength of one and the maximum of the electric field in the cavity is 36. The contour plot focuses in on the area surrounding the post in such a way that the scaling between the z and x axis are in one-to-one correspondence. The convergence time for this simulation was 635 min. Again, this convergence time is large because a fine mesh (i.e., small Δ) is needed for the stringent converge of the electromagnetics fields to ensure that the cavity is resonant. To check these results and compare convergence times, we applied the FDTD to the same scattering problem with the iris present. The results were identical to the hybrid method. However, the convergence time was 5060 min, a factor of roughly 8 times slower.

6. CALCULATION OF RESONANT LENGTHS

The hybrid method described in this paper requires an extremely accurate approximation of the resonant length of the cavity. This critical length depends upon the size of the aperture and upon the geometry and electrical permittivity of the ceramic. The technique we now develop to determine this critical length is again based upon scattering matrix theory.

We begin by considering the scattering problem shown in Fig. 7 where E_0 is the amplitude of the incident mode. The short has been removed for the moment. We again place a imaginary plane at $z = z_I$. Focusing our attention to the left of this plane, the iris again is irradiated by two modes of strength E_0 and E_1 and reflects two modes of strengths R_0 and T_1. These coefficients are related by Eqs. (10).

Next we consider the region to the right of $z = z_I$. If we irradiate the ceramic by two incident modes of strengths E_2 and E_3 and denote their reflected mode amplitudes by R_2

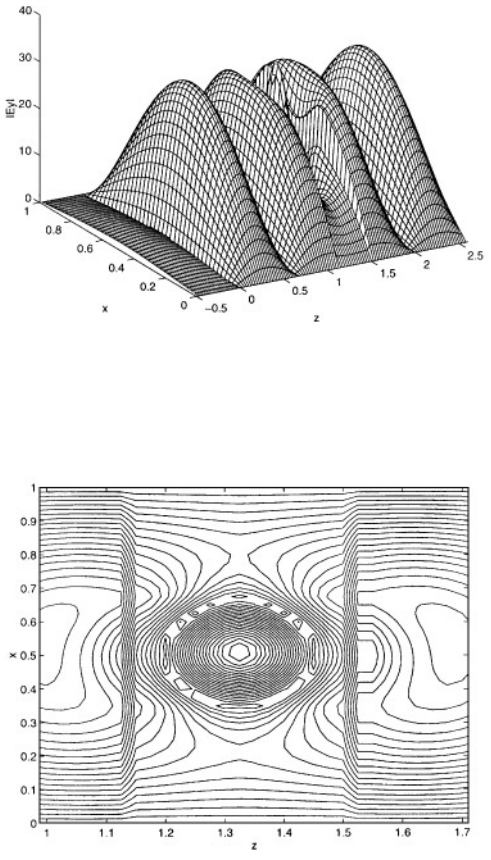

FIG. 6. Amplitude of E_y throughout the TE_{103} waveguide applicator containing a post with $\sigma = 0$.

and R_3, respectively, then these amplitudes are related by

$$R_2 e^{-ik_1 l/2} = r_c E_2 e^{ik_1 l/2} + t_c E_3, \tag{22a}$$

$$R_3 = t_c e^{ik_1 l/2} E_2 + r_c E_3. \tag{22b}$$

Here r_c and t_c are the reflection and transmission coefficients caused by an incident mode of unit strength when the cylinder is located at $z = 0$ in an otherwise empty and homogeneous infinite waveguide. The cylinder is assumed to be symmetric about the point $z = 0$.

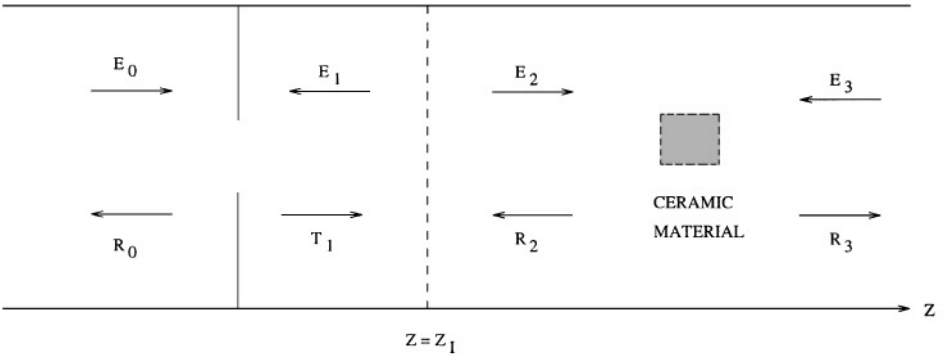

FIG. 7. Scattering matrix schematic for resonant length calculation.

These coefficients depend upon the geometry and permittivity of the ceramic and are obtained numerically. If we only send a mode of unit amplitude in from the left, then we can use the FDTD technique described in this paper to compute r_c and t_c. However, we must now truncate the numerical domain on the right at $z = z_r$; this boundary is chosen far enough to the right of the cylinder to neglect evanescent modes. Then the appropriate non-reflecting boundary operator is [15]

$$\frac{\partial E_y}{\partial z} + k_1 \frac{\partial E_y}{\partial t} = 0. \tag{23}$$

The coefficients r_c and t_c are obtained from this numerical calculation. When the ceramic contains no loss, power is conserved and these coefficients obey the relationships

$$|r_c|^2 + |t_c|^2 = 1 \tag{24a}$$

$$\text{Real}(r_c t_c^*) = 0. \tag{24b}$$

When r_c and t_c are determined numerically, these relationships are not satisfied exactly. This limits the accuracy of the calculation of the resonant length. Therefore, in the calculations which follow, we take r_c to be the value determined numerically and take t_c to be the value which allows these relationships to be satisfied exactly. That is,

$$t_c = \sqrt{1 - |r_c|^2} e^{i[\frac{\pi}{2} + ph(r_c)]}, \tag{25}$$

where $ph(r_c)$ is the phase of r_c.

We now connect these two problems at the plane $z = z_I$. There we observe that the incident mode (from the right) on the iris is the reflected wave off the post. Equating modal amplitudes we find $E_1 = R_2$. Similarly, the mode reflected by the iris to the right is the incident mode on the cylinder. Thus, we have $T_1 = E_2$. Finally, if the short is placed at $z = l/2$ and the cylinder located at $z = 0$, then R_3 and E_3 are related by $E_3 = \Gamma(l) R_3$. Here $\Gamma(l) = -\exp(ik_1 l)$ the reflection coefficient from the short. Combining these results with Eq. (22) gives $E_1 = \gamma_1 T_1$ where

$$\gamma_1 = \left(\frac{r_c + (r_c^2 - t_c^2) e^{ik_1 l}}{1 + r_c e^{ik_1 l}} \right) e^{ik_1 l}. \tag{26}$$

This is the reflection coefficient for a loss-less post located at $z = l/2$ in a homogeneous waveguide with a short at $z = l$. It follows from this expression and Eq. (24) that $\gamma_1 = e^{i\theta}$, i.e., it is a complex number of unit amplitude.

The resonant length of the cavity will be length which maximizes $|T_1|$. From Eq. (12), it is apparent that this maximum value corresponds to the minimum value of $|1 - r_1 \gamma_1|$. Using the approximation for r_1 in Eq. (11), we find that $|T_1|$ will be maximum in value when θ is given by

$$\theta_M = \pi - \tan^{-1}(1/S). \tag{27}$$

The value of its maximum is

$$|T_1| = (1 + 2S^2 - 2S\sqrt{1 + S^2})^{-1/2} \tag{28}$$

which for small apertures ($S \gg 1$) is approximated by

$$|T_1| = 2S. \tag{29}$$

Setting $\gamma_1 = e^{i\theta_M}$, with θ_M given by Eq. (27), inserting this result into Eq. (26), and solving for l we obtain

$$l = \text{Real}\left(\frac{\ln(u)}{ik_1}\right), \tag{30}$$

where

$$u = \frac{-r_c(1-e^{i\theta_M}) - \sqrt{r_c^2(1-e^{i\theta_M})^2 + 4\left(r_c^2 - t_c^2\right)e^{i\theta_M}}}{2\left(r_c^2 - t_c^2\right)}.$$

7. CONCLUSIONS

A hybrid numerical method was developed for describing the interaction of an electromagnetic wave with a low-loss ceramic material in a high Q cavity. The method utilizes a combination of asymptotic and numerical techniques. The resultant hybrid method was used on two example problems: a slab and a post. It was found for these cases to be approximately six times faster than a straightforward application of the FDTD method. This difference would become even greater if the aperture were made smaller than 17.5 mm. However, both our hybrid method and a straightforward application of the FDTD method to the full problem suffer from the requirement that an extremely accurate estimate of the resonant length (frequency) is required. When the Q of the cavity is extremely large, then an error of magnitude Δ in the resonant length l may detune the cavity and yield $O(1)$ electric fields. Clearly, this scenario will defy any method.

It is worthwhile to point out that the numerical component of our hybrid scheme is not bound to the FDTD method. Other numerical methods, such as finite element methods or any elliptic solver, can be used.

ACKNOWLEDGMENTS

This effort was sponsored by the National Science Foundation under Grants DMS 9407196 and DMS 9623543, the Department of Energy under Grant DEFG0294ER 25196, the New Jersey Institute of Technology under Grant 421070, and the Air Force Office of Scientific Research, Air Force Material Command, USAF, under Grant F49620-96-1-0039. The U.S. Government is authorized to reproduce and distribute reprints for governmental purposes notwithstanding any copyright notation therein. The views and conclusions contained herein are those of the authors and should not be interpreted as necessarily representing the official policies or endorsements, either expressed or implied, of the Air Force Office of Scientific Research or the U.S. Government.

REFERENCES

1. K. S. Yee, *IEEE Trans. Anttennas Propag.* **AP-14**, 302 (1996).
2. M. F. Iskander, *IEEE Trans. Microwave Theory* **42**(5), (1994).
3. J. Wei, M. Hawley, and J. Asmussen, *J. Micro. Power* **28**(4), 234 (1993).
4. C. S. Morawetz, *Comm. Pure Appl. Math.* **15**, 181 (1962).
5. D. C. Dibben, W. B. Fu, and A. C. Metaxas, *Mat. Res. Soc. Symp. Proc.* **347**, 305 (1994).

6. T. A. Grotjohn and J. Asmussen, *Mat. Res. Soc. Symp. Proc.* **430**, 357 (1996).
7. J. A. Pereda, L. A. Viela, and A. Prieto, *IEEE Microwave Guided Wave Lett.* **2**, 431 (1992).
8. L. Lewin, *Theory of Waveguides* (Wiley, New York, 1975).
9. J. M. Neilson, P. E. Latham, M. Caplan, and W. Lawson, *IEEE Trans. Microwave Theory* **37**(8), (1989).
10. J. E. Labaric and D. Kajfez, *IEEE Trans. Microwave Theory* **37**(11), (1989).
11. B. Chapman, M. F. Iskander, R. L. Smith, and O. M. Andrade, *Mat. Res. Soc. Symp. Proc.* **269**, 53 (1992).
12. T. F. Chan and T. P. Mathew, *Acta Numerica 1994* (Cambridge Univ. Press, Cambridge, UK, 1994).
13. T. W. Huang, B. Houshmand, and T. Itoh, *IEEE Microwave Guided Wave Lett.* **3**, 378 (1993).
14. T. W. Huang, B. Houshmand, and T. Itoh, *IEEE Trans. Microwave Theory* **42**, 2149 (1994).
15. G. A. Kriegsmann, *SIAM J. Sci. Stat. Comput.* **3**(3), 318 (1982).
16. G. A. Kriegsmann, *SIAM J. Appl. Math.* **57**(2), 382 (1997).
17. A. Taflove, *Computational Electrodynamics: The Finite-Difference Time-Domain Method* (Artech House, Norwood, MA, 1995).
18. K. Kunz and R. Luebbers, *The Finite Difference Time Domain Method for Electromagnetics* (CRC Press, Boca Raton, FL, 1993).